Original Article: Evaluation of V2G System in Electric Vehicle and DC Charging System

Ebadollah Amouzad Mahdiraji

Department of Engineering, Sari Branch, Islamic Azad University, Sari, Iran

Use yor device to scan and read the article online

Citation: E. Amouzad Mahdiraji, **An Overview of Methane Gas Hydrate Formation**. J. Eng. Indu. Res., **2021**, 2(3):178-193.

http://doi.org/10.22034/jeires.2021.278468.1034

Article info:
Received: 25 November 2020
Accepted: 04 April 2021
Available Online: 04 May 2021
Checked for Plagiarism: Yes
Peer Reviewers Approved by:
Dr. Amir Samimi
Editor who Approved Publication:
Professor Dr. Mohammad Haghighi

Keywords:
V2G system, Electric Vehicle, Intelligent power grid, Particle Swarm Optimization algorithm (PSO), Economic dispatch.

ABSTRACT

With an increasing number of electricity companies' subscribers, the necessity of restructuring these systems has become an important issue that cannot be overlooked. Therefore, a solution that has become interesting subject for network designers is the evolution of the traditional power grids into intelligent power grids. One of the influential elements in these networks is electric vehicles, which are considered by both researchers and consumers. They are eco-friendly and provide the needed comfort. Given the fact that the presence of these vehicles is growing in the networks, an important challenge which is posed is their exploitation as an actor in the secondary services market of the power networks. So, it is possible to achieve peak shaving in the power system by optimally scheduling the charging and discharging time of these vehicles. In this paper, PSO and ACO algorithms were used as optimizing tools for charging and discharging time of the vehicles and then the DVR was applied as the stabilizer of the network asymmetry.

Introduction

The distributed storage technology, like vehicle-to-grid (V2G) system, is a promising technology for the load balancing in the future due to its fast response feature and high storage potential. Considering the energy vision in 2011, the share of oil consumed in the transportation sector increased from 40% in 2008 to 54% [1-7]. On the other hand, the International Energy Agency's (EAI) forecasts indicated an increase in oil prices to 5.5$ per gallon at the highest possible rate. Technologies that reduce fuel consumption in the transportation sector, such as the hybrid electric vehicle (PHEVs) and the vehicle-to-grid (V2Gs), have increased their position among other ones. In the coming years, many vehicles are expected to have a plug-in option to charge their batteries, and by 2030, the development of V2Gs will have reached 25% [8-12]. Electric vehicles can charge their batteries in any situation. Many

Corresponding Author: *Ebadollah Amouzad Mahdiraji, (ebad.amouzad@gmail.com)*

researchers have studied the electric vehicles' optimal capacity and location of the parking lots and charging stations. With the V2G, an opportunity to design a two-way charging with the performances such as active filters in the micro-grid power network can be provided. V2Gs can participate in the secondary services market as spinning reserves [13-15], regulator [16-19], storage system for renewable energy sources [20-23], and reactive power compensators to increase power quality [24]. According to the electricity pricing model, V2Gs can affect load curve charges. There are a lot of challenges for using these vehicles on a large scale. Although the cost of these cars is lower, they still continue to have a higher initial cost than combustion engine vehicles. In addition, access to charging station is limited and much investment is required to create charging stations. Also, electric vehicles receive a lot of energy from the network at the time of charging. Therefore, uncoordinated charging of a large number of electric vehicles can have adverse effects on it, i.e., power outage, non-volatile oscillation. To meet the peak demand of electric vehicles, increasing the power generation can be one of the possible solutions, although this will cost a lot. One of the solutions, which is cost-effective, is also the coordinated charging of the electric vehicles that makes it easier to adjust frequency and optimize the use of the power generation.

The aim of this study was providing an optimal charging and discharging scheduling of V2Gs and applying them as the equipment used to adjust peak demand of the power network. In other words, attempts were made to provide the maximum adjustment times of peak demand by offering an accurate charging and discharging schedule for V2Gs. In the present paper, an Ant Colony Optimization (ACO) algorithm and Particle Swarm Optimization (PSO) algorithm were used to find a way to optimize the charging and discharging of electric vehicles [25-27].

Electric load flow problem

In this paper, Particle Swarm Optimization (PSO) and Ant Colony Optimization (ACO) algorithms were described, since two optimization problems were concerned. These two problems are the optimization of the charging and the discharging schedule of the eclectic vehicles and the economic dispatch (ED). In fact, in order to solve the problem of optimal scheduling of the units, ED must be continuously implemented and an optimal arrangement of the power purchases for units be provided[28].

The simulation problem model

In this part, the problem of charging and discharging of the electric vehicles during a day and night with a load pattern is given in Table 1 and Figure 1. Note that the amount of the given consumption is in kilowatt-hour.

Table 1. Charging and discharging of the electric vehicles during a day and night with a load pattern

Hour	Load amount	Hour	Load amount	Hour	Load amount	hour	Load amount
1	700	7	1150	13	1400	19	1200
2	750	8	1200	14	1300	20	1400
3	850	9	1300	15	1200	21	1300
4	950	10	1400	16	1050	22	1100
5	1000	11	1450	17	1000	23	900
6	1100	12	1500	18	1100	24	800

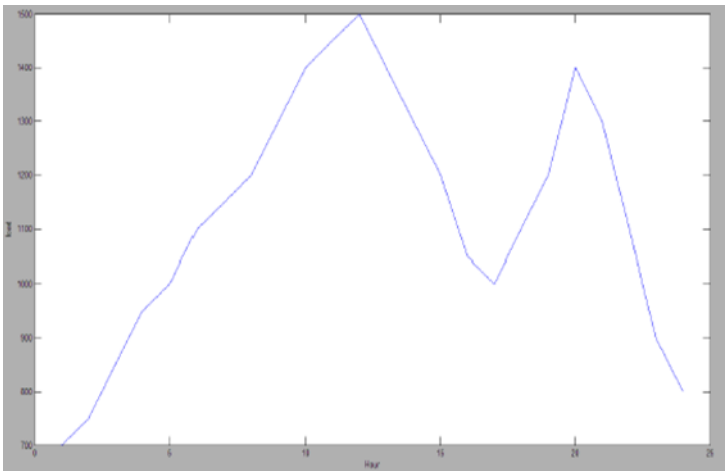

Figure 1. The graph of consumption pattern during a day and night

As can be seen, Figure 1 displays the consumption pattern in 24 hours, the peak time occurs at two points, in which the algorithm is required to perform the peak adjustment process by providing a charging and discharging scheduling arrangement of the electric vehicles. It should be noted that the peak adjustment can be done based on the three general approaches, including load shifting, peak clipping, and valley filling; the general schema of the used method is depicted in Figure 2 below. The applied method in the present article is the load shifting technique.

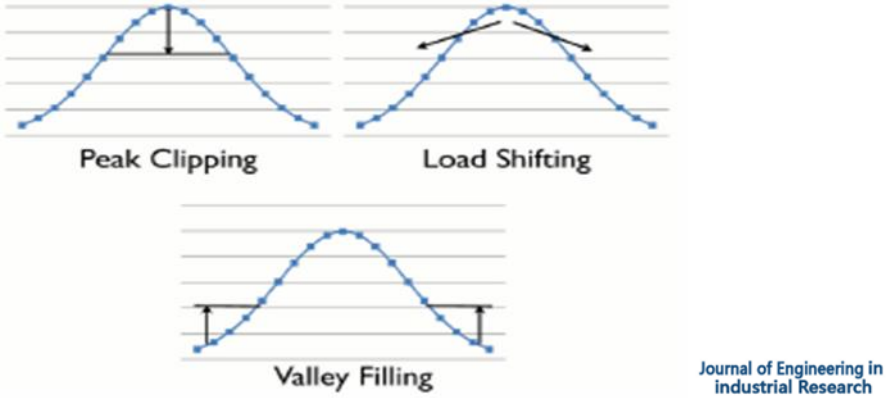

Figure 2. Peak adjustment techniques in power network

Reviewing and evaluating of the desired simulation

In order to provide an optimal model of the system, 20 V2Gs were assumed, and a certain power was considered for each one. Because of the dual nature of the consumer and the generator of the electric vehicles, it is clear that in order to find a solution, we face two optimization problems, namely the Economic Dispatch (ED) and vehicle coordination problems. In other words, ED is used to plan the amount of the received power from the electric vehicles and another algorithm is used to schedule their discharging. To solve the first problem (economic dispatch problem) and the second problem (discharging coordination problem) ACO algorithm and PSO algorithm were used, respectively. In order to find the optimal solution of the planning problem using the PSO algorithm, in the first step, 10 seeker particles in 30 iterations were considered, and to solve the ED scheduling problem using an ACO algorithm, 10 ants searched the solution in 100 iterations. The obtained simulation result is presented in Figure 3 [29-31].

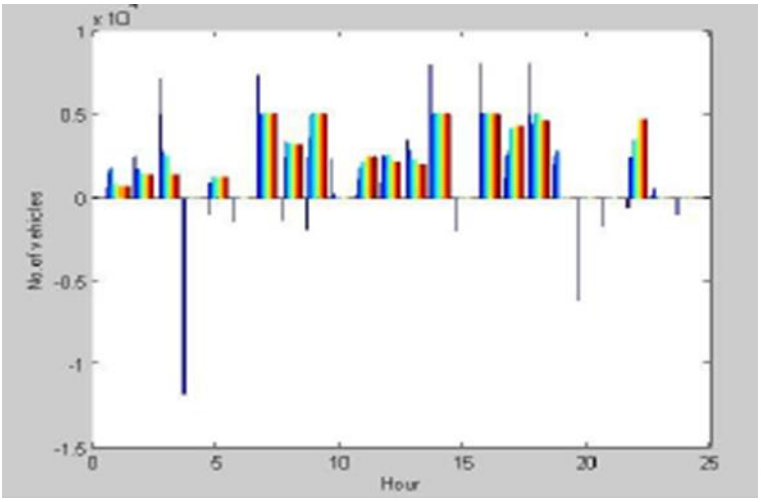

Figure 3. Charging and discharging graph of each vehicle per hour

Figure 3 illustrates the charging and discharging of vehicles and their time. As can be seen, the upper part of the diagram shows the amount of the vehicles' discharging and the lower part of this axis represents the charging time of each vehicle [32-34].

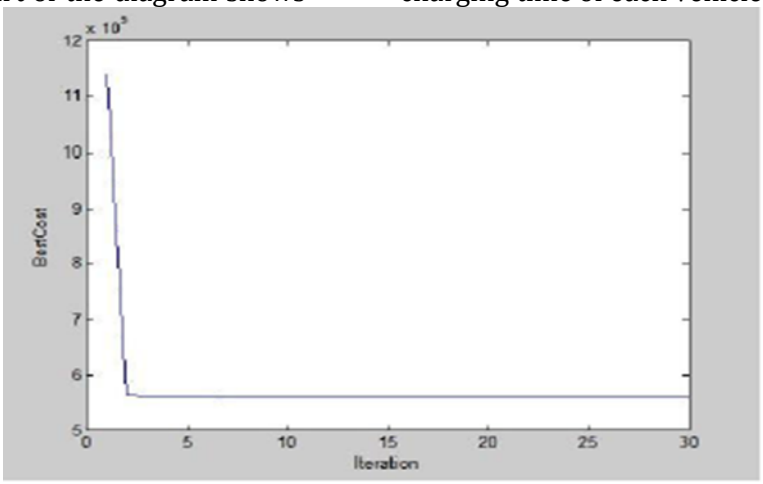

Figure 4. The cost function graph in terms of the iteration numbers

Figure 4 displays the optimized cost of the objective function by the optimization algorithm that, because of the execution of only 30 iterations, the algorithm still looks for better responses. In the second step, 20 seeker particles in 50 iterations were considered and for solving the ED scheduling problem, using an ACO algorithm, 20 ants in 100 iterations searched the optimal response. The simulation results were obtained as follows [34-36].

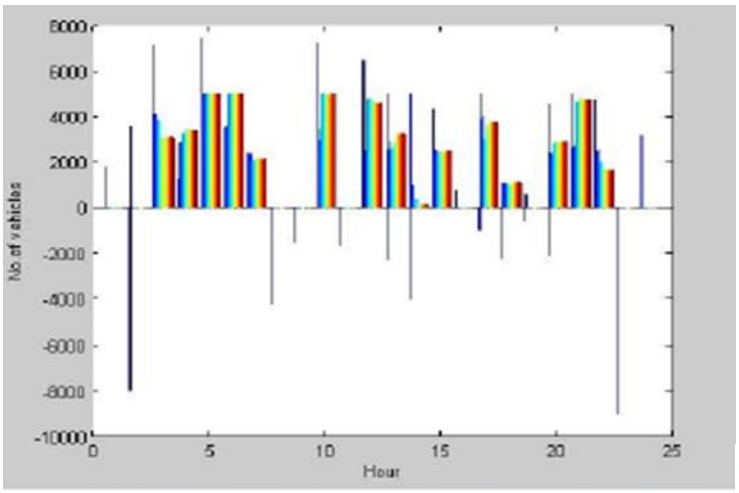

Figure 5. Charging and discharging graph of each vehicle per hour

In Figure 5, as can be seen, the part of the graph that appears at the top of the time axis represents the amount of the discharging toward the network and the lower part of this axis represents the charging time of each vehicle

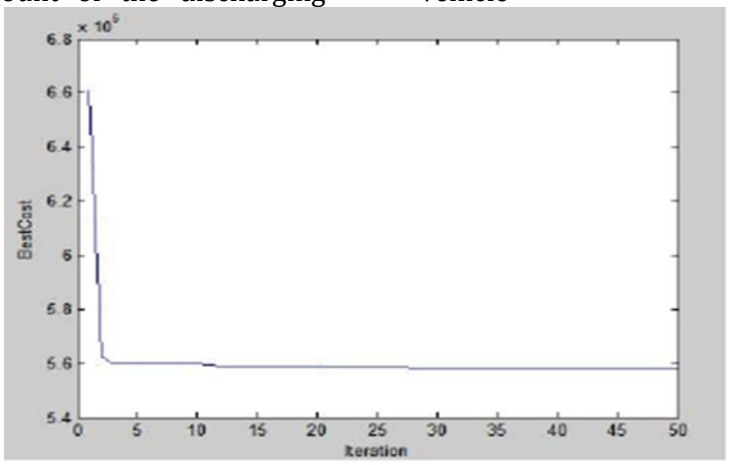

Figure 6. The cost function graph in terms of the iteration numbers

Figure 6 shows the optimized cost of the objective function using the optimization algorithm that, because of the execution of only 50 iterations, the algorithm still looks for better responses. In the third step, in order to solve the optimal scheduling problem, the PSO algorithm with 50 seeker particles in 200 iterations was considered. On the other hand, for solving the ED scheduling problem, using an ACO algorithm, 50 ants in 100 iterations searched the optimal response. The simulation results obtained as follows.

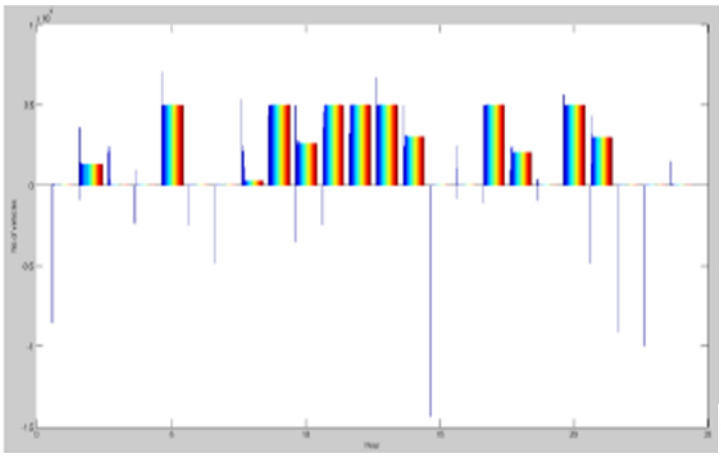

Figure 7. Charging and discharging graph of each vehicle per hour

As shown in figure 7, the upper part of the time axis in this graph represents the amount of the vehicle discharging toward the network and the lower part of this axis displays the charging time of each vehicle. It is worth mentioning that, the presented graph in this section is for 50 ants in 100 iterations, which caused a non-exact matching with the load pattern.

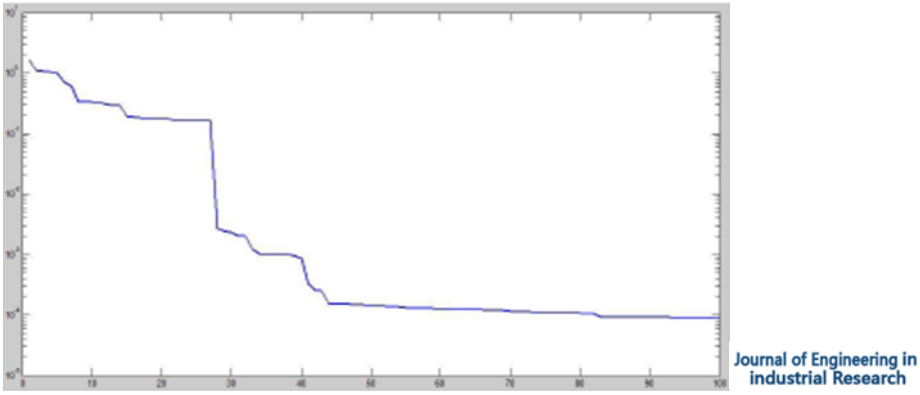

Figure 8. The cost function graph in terms of iteration numbers

As evident from Figure 8, this graph shows the optimized cost of the objective function using the optimization algorithm; because of execution of only 100 iterations, the algorithm continues to look for more optimal responses. It should be noted that the reason for the implementation of simulation up to 100 iterations is the amount of data being processed, for which their execution requires a lot of time. According to the aforementioned issues, an important point that is well known in this area is the creation of imbalance on the three-phase network due to the asymmetric presence of these vehicles on the different phases as load. In fact, by coordinating charging and discharging of the vehicles in order to adjust the peak, the indicators of the network power quality should not be overlooked. However, here it is necessary to use FACTS devices such as DVR, STSTCOM, SVC, or SSSC to improve the network reliability indices. In this paper, after charging and discharging scheduling of the vehicles, the Dynamic Voltage Restore (DVR) was used to improve the power quality of the network. The reasons for choosing DVR are the low occupation amount of these devices, non-complexity of the control system, cost-effectiveness, and proper small-scale performance. The presence of DVR in the network results in correcting the sudden voltage collapse caused by sudden vehicle entrance into the network and protecting the main network.

Device description and simulation model

In general, to implement the proposed power system models, SIMULINK/MATLAB software environment can be regarded as one of the most powerful simulation software for analyzing the results of the model. In this paper, this software was used to analyze the proposed idea and it was tried to provide a general model of a power grid to evaluate the selected strategy for controlling DVR devices and it was attempted to show that this model could be the most effective method for reducing the voltage drop in distribution networks with sensitive loads.

The simulated system profiles

To model the proposed control system, a general schema of the implemented model in MATLAB/SIMULINK environment is presented.

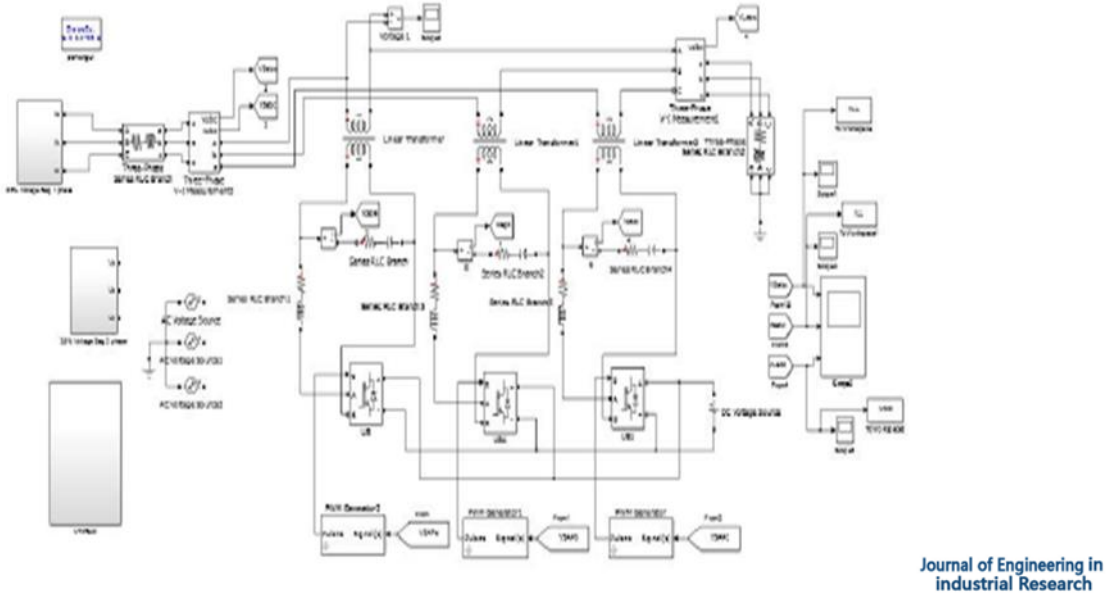

Figure 9. The general schema of the simulated circuit in SIMULINK/MATLAB environment

In order to analyze the proposed idea, it is necessary to implement a model in SIMULINK environment, according to Figure 9. Since the purpose is to investigate the effect of the DVR on the voltage drop reduction, hence for modeling the desired problem in the network input, a feeder is considered, which at a moment of 0.1 second, the output of the phase a has a drop of 35% of the amplitude than the other two phases. The block placed in the input of the circuit, as shown in Figure 10, is responsible for producing such a situation for the system.

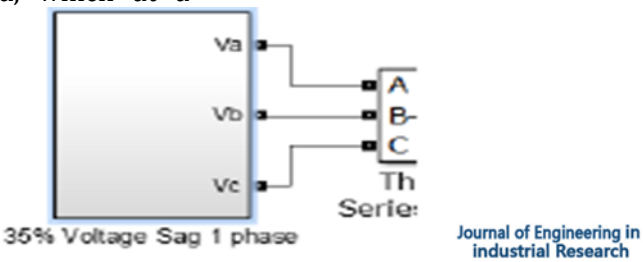

Figure 10. The voltage generator block having a drop of 35% in phase a

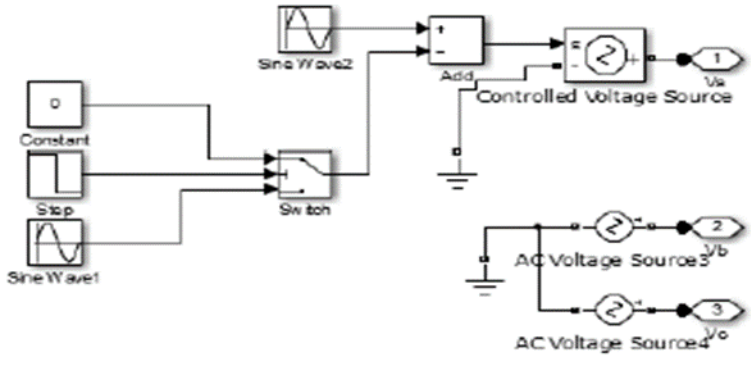

Figure 11. The generator circuit with a voltage drop of 35% of the phase a

Figure 11 shows the internal circuit of the block (10). As can be seen, in this circuit, two phases of b and c, having equal amplitudes, begin to work with the phase differences of -120 and +120, respectively, as well as a phase with difference 0 degrees having an equal amplitude of two other phases. After 0.1 second, a sudden voltage drops of 35% of the voltage amplitude of the phase a occurs and this voltage is applied to the load.

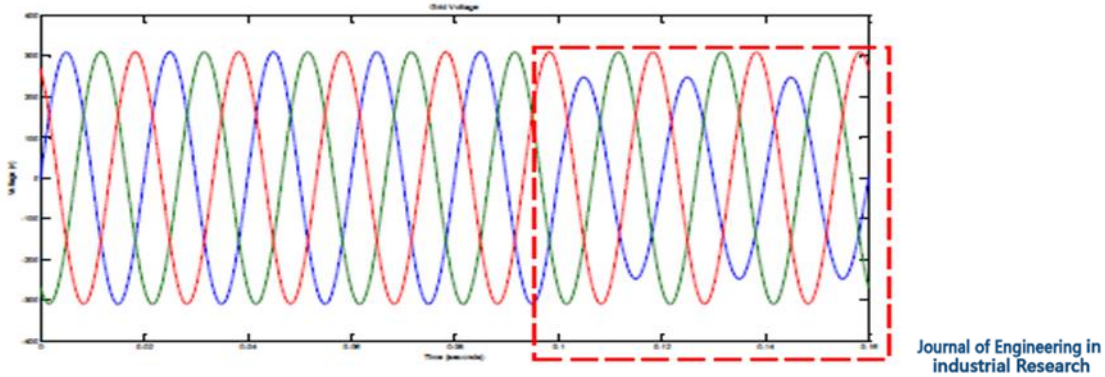

Figure 12. Circuit input voltage diagram

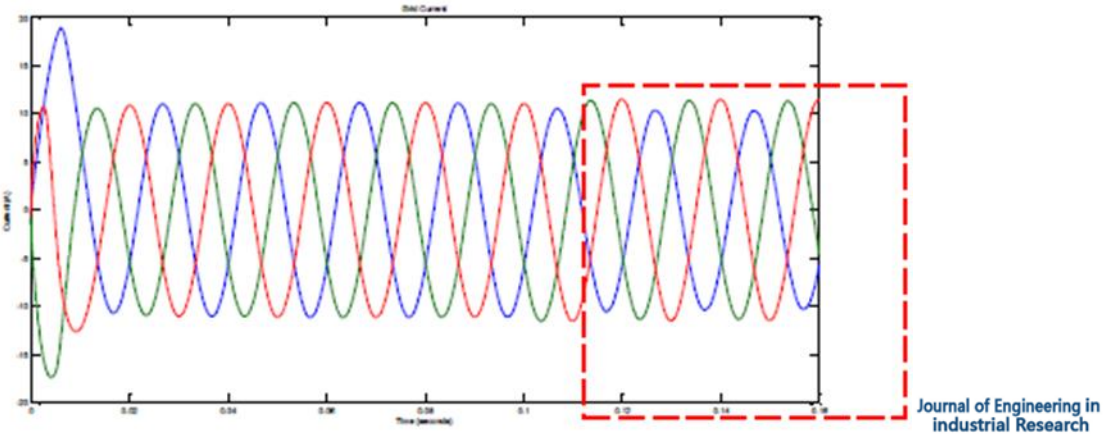

Figure 13. The corresponding flow diagram in accordance with the input voltage sag

If the generated voltage directly connects to the load, the load will also receive this voltage drop and will be in trouble. Here, using the DVR control circuit, the voltage can be restored to the initial balance at the terminals of the load. Figure 15 shows the three-phase voltage diagram in the load terminal after the compensation. Figure 14 displays three linear transformers of two coils, the outputs of which are sequentially and one-to-one with the

phases a, b, and c of the circuit. Three inverters are also used in this circuit, which are IGBT/Diods series and are powered by a DC source. Its internal structure is shown in Figure 16.

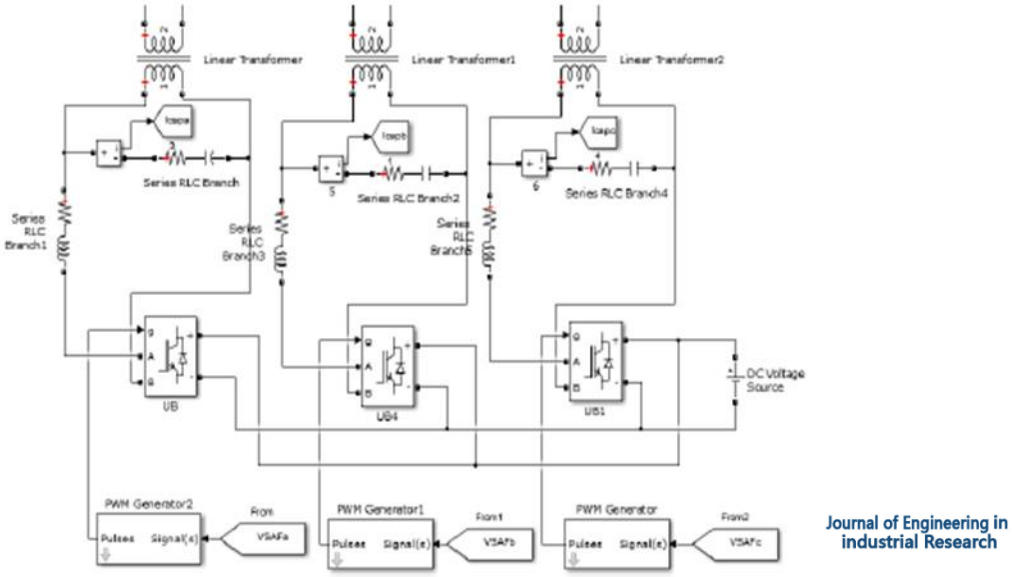

Figure 14. Control circuit diagram of DVR compensation circuit

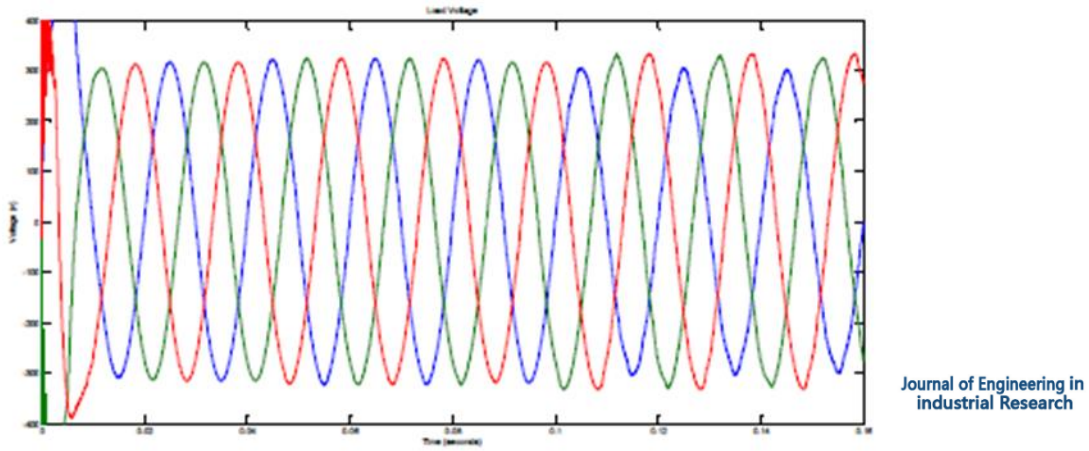

Figure 15. The diagram of the load terminals voltage after compensation by the DVR system

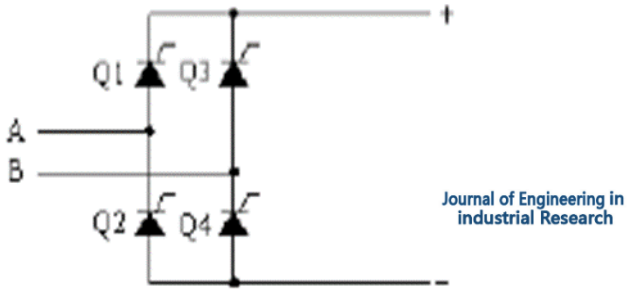

Figure 16. Internal circuit of inverter bridge

As shown in Figure 14, parallel filters were used at the both ends of the control circuit to optimally prevent the injection of the voltage harmonics into the circuit. It should be noted

that the load characteristic used in this simulation is a parallel inductive-resistive to ground load with a resistor and inductor of 24 Ohms and 50 mH, respectively.

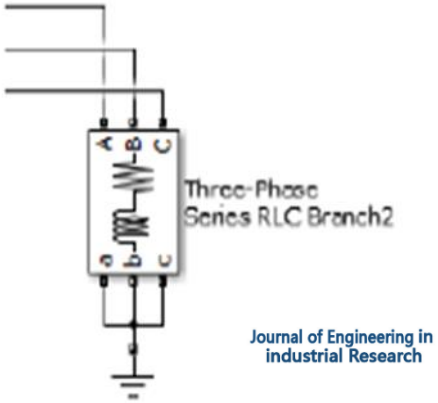

Figure 17. Used topology in design

Describing the operation of the control circuit

In order to illustrate the operation of the control circuit, at first the schema of the proposed system is presented in Figure 18. As can be seen, this circuit consists of four basic components, each of which has a specific task. These four sections consist of a part that transforms abc load and input source components to dq components, the RDC block, the FFC block, and a part which sends the output signals to the control terminals.

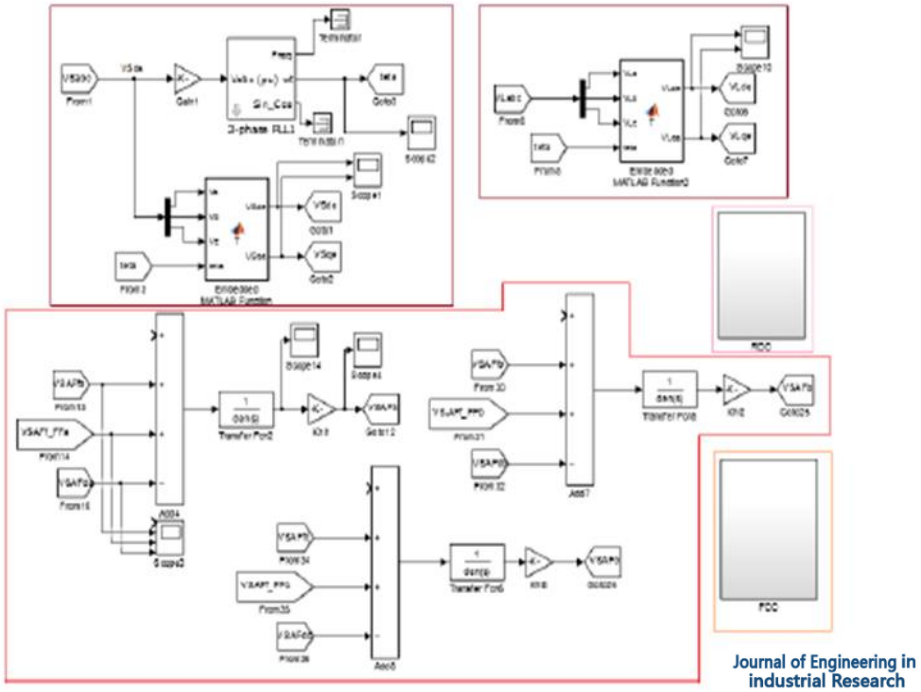

Figure 18. The circuit of DVR control system

First, in the abc to dq transformation circuit, the abc three phase vectors are determined by the PLL, and then are prepared as dq vectors. This transformation coincides with the input voltage signal and load. When the dq component of the load and input are extracted, these controllers enter the FCC and the internal circuit of FCC controller is shown in Figure 19.

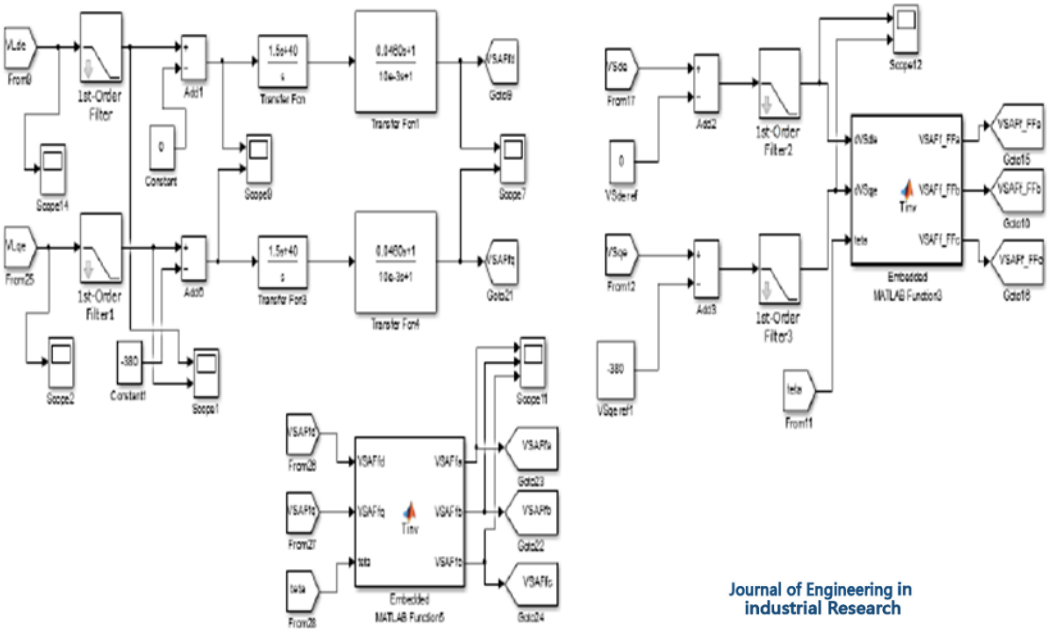

Figure 19. The internal circuit of the FCC controller block diagram

In this controller, as can be seen, in order to measure the voltage difference over the values of the main component, they are transmitted through a low-pass filter, after that the difference is calculated from its base value, and eventually it is modeled by passing through the PI controller. The diagram of the output signal scope7 is illustrated in Figure 20.

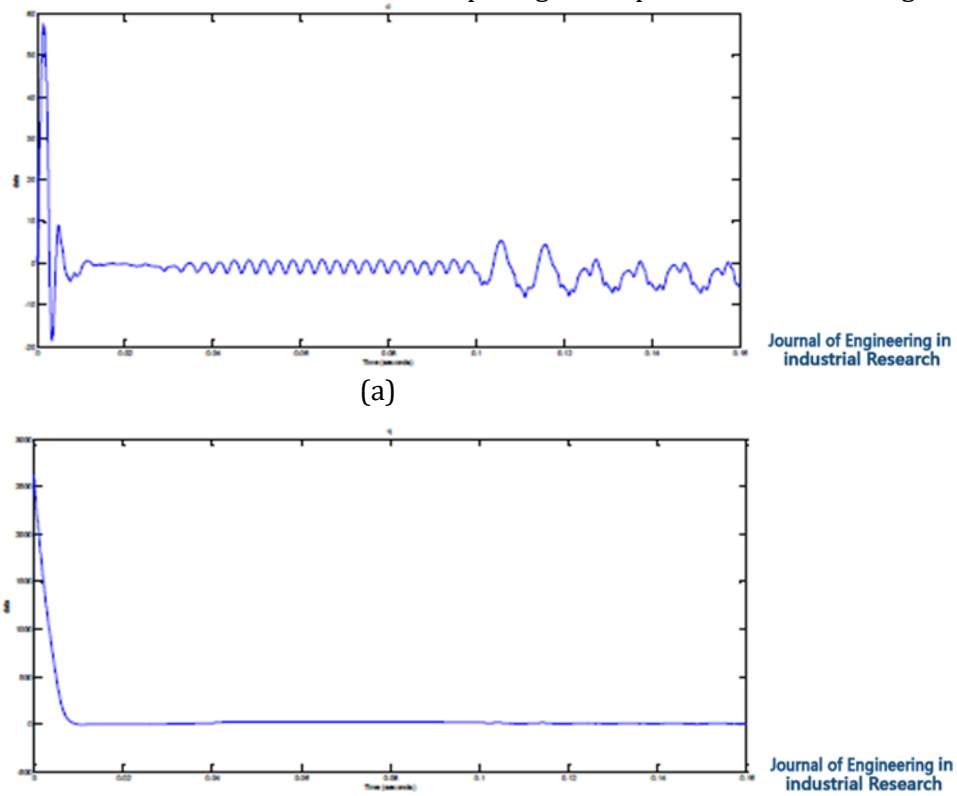

Figure 20. The diagram of the output voltage waveform from the controller as d component (a), the diagram of the output voltage waveform from the controller as q component

The outlined steps are also the same for the input signal. These signals in scope12 are shown in Figure 21.

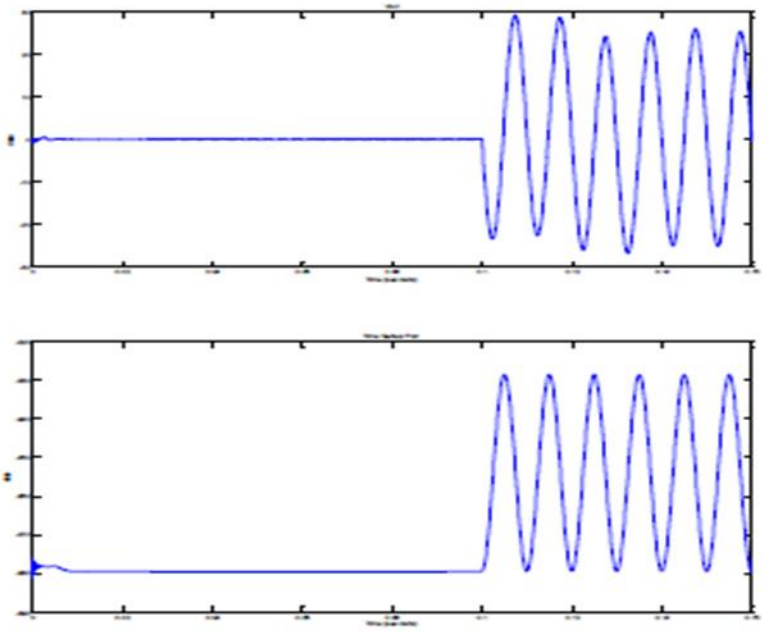

Figure 21. The diagram of the input signal format was excluded out of the controller

Finally, after applying the control operations on the input and load signals, they are again extracted as abc components. A capacitor-current-feedback coupled with an impact factor in the RDC block was used to reduce the voltage oscillation of the filter capacitor voltage. The internal structure of this bock is shown in Figure 22 [37].

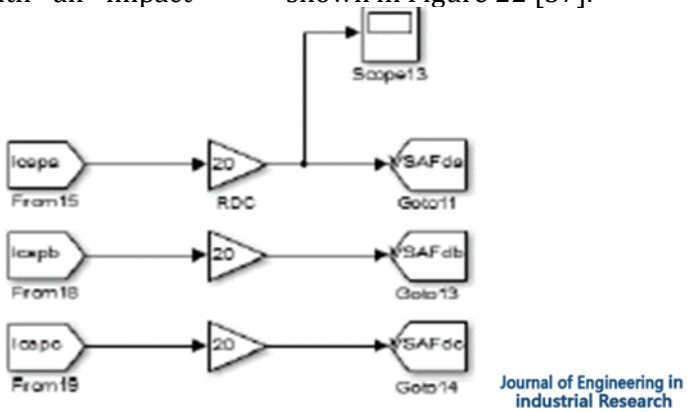

Figure 22. The internal structure of the RDC block

At last, by controlling three generated control signals produced in two blocks of FFC and RDC blocks and a transition, a post-phase block is used. All the above steps, by placing and integrating in the controller circuit, provide the output results represented in Figure 23. Figure 23 is a combination of three waves indicating the input voltage, current, and the compensated load voltage.

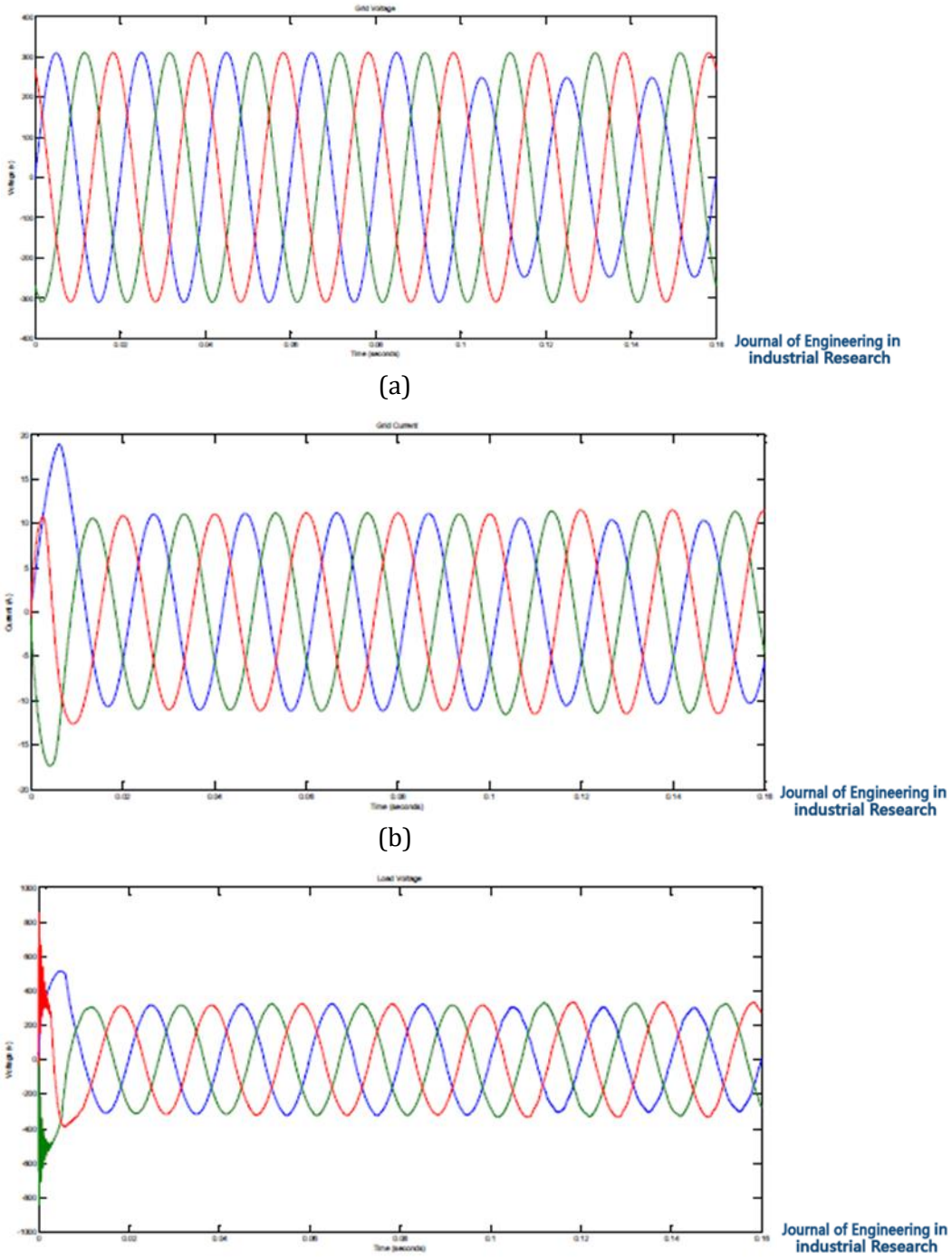

Figure 23. Input voltage waveform (a), the current after compensation (b), voltage after compensation (c)

Similar to the studies of single-phase voltage drop, in the case of a three-phase voltage drop the expected results can also be extracted. In this case, the input source is designed as shown in Figure 24. This design models a 35% voltage drop-down at 0.1 second.

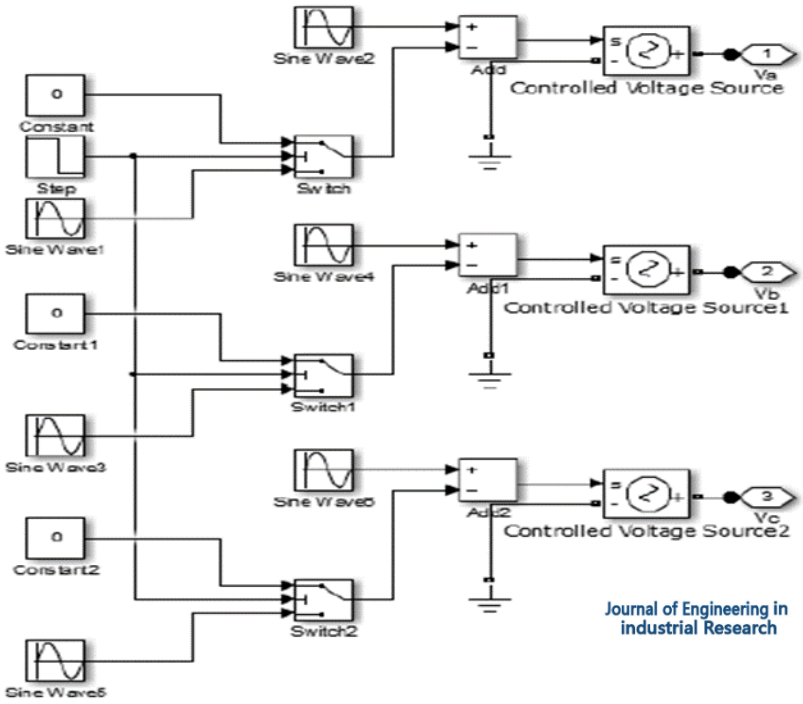

Figure 24. The internal structure of the input source feeder which models the voltage drop-down

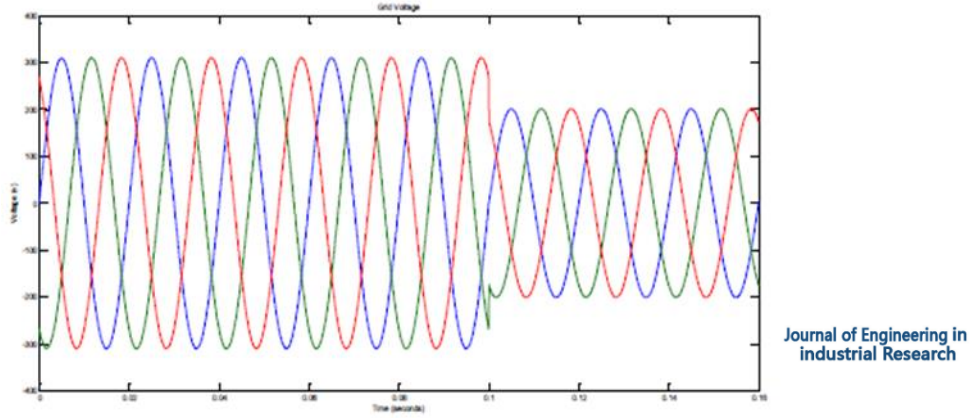

(a)

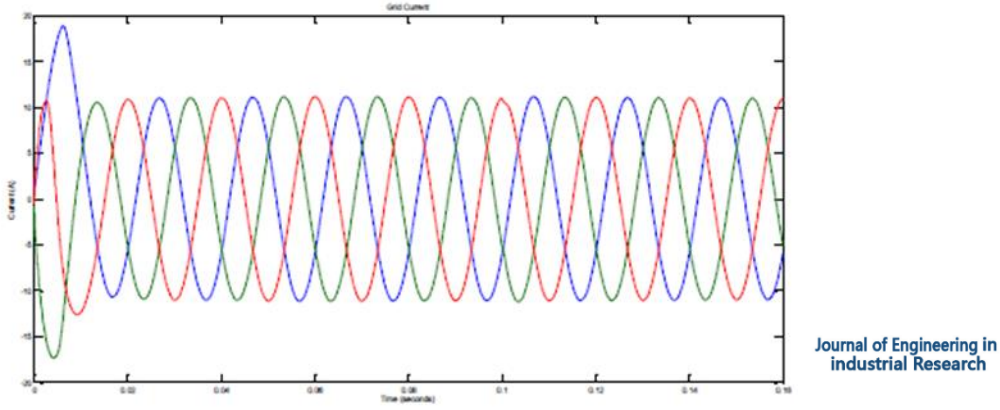

(b)

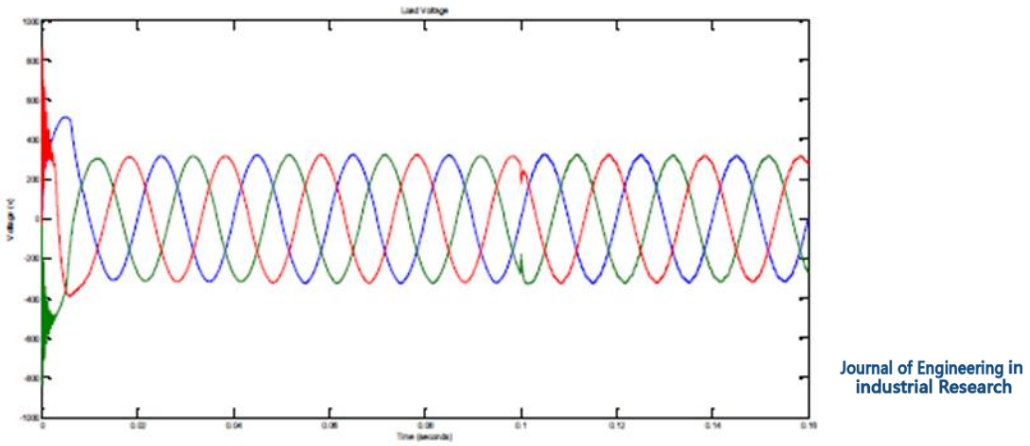

(c)

Figure 25. Input three-phase voltage waveform (a), the three-phase current after compensation (b) the three-phase voltage after compensation (c)

Results

In different sections of this paper, the control methods, exploitation, and optimal coordination of electric vehicles were presented. It was shown that the proposed method for maximizing the use of the electric vehicles could help to smooth the load pattern of distribution networks. The simulation results were analyzed for a conventional load during a day and night and it was shown that the proposed idea has a proper quality to smooth the load pattern of distribution networks. The discussed idea is for scheduling the time and the amount of charging and discharging of 20 V2Gs that by optimally coordinating them, it is possible to maximize the peak adjustment and/or shift the peak hours to off-peak times.

Orcid

Ebadollah Amouzad Mahdiraji:
https://orcid.org/0000-0003-3777-4811

References

[1] E. Amouzad Mahdiraji, S. Shariatmadar, *International Journal of Smart Electrical Engineering*, **2019**, 8, 99-104.
[2] E. Amouzad Mahdiraji, S. Shariatmadar, *International Journal of Smart Electrical Engineering*, **2019**, 8, 51-58.
[3] P.J. Bree, A. Veltman, V.D. Bosch, *Vehicular technology*, **2009**, 2, 58, 588-595.
[4] E. Amouzad Mahdiraji, A. Yousefi Talouki, *Journal of Chemical Reviews*, **2020**, 2, 284-291.
[5] E. Amouzad Mahdiraji, S. Shariatmadar, *International Journal of Smart Electrical Engineering*, **2019**, 8, 143-148.
[6] E. Amouzad Mahdiraji, S.M. Shariatmadar, *Advanced Journal of Science and Engineering*. **2020**, 1, 27-31.
[7] W. Li, *John Wiley & Sons*, **2005**, 1, 108-164.
[8] E. Amouzad Mahdiraji, M. Sedghi Amiri. *International Journal of Smart Electrical Engineering*, **2020**, 9, 01, 13-21.
[9] E. Amouzad Mahdiraji, *Journal of Scientific Perspectives*, **2020**, 4, 245-254.
[10] E. Amouzad Mahdiraji, M. Amiri, *Journal of Engineering Technology and Applied Sciences*, **2020**, 5, 133-147.
[11] J. Lei, J. Xie, D. Gan, *Automation of power system*, **2009**, 4, 23, 33-35.
[12] E. Amouzad Mahdiraji, *Gazi Mühendislik Bilimleri Dergisi (GMBD)*, **2020**, 6, 138-144.
[13] E. Sortomme, M.A. El-Sharkawi, *IEEE Trans. Smart Grid*, **2011**, 2, 131–138.
[14] E. Amouzad Mahdiraji, *Transactions of Electrical, Electronic and Computer Engineering* **2020**, 6, 238–244.
[15] E. Amouzad Mahdiraji, A. Yousefi Talouki, *Journal of Chemical Reviews*, **2021**, 3, 40-49.
[16] K. Clement-Nyns, E. Haesen, J. Driesen, *IEEE Trans. Power Syst.*, **2010**, 25, 371–380.

[17] Y. Raziani, S. Raziani, *International Journal of Advanced Studies in Humanities and Social Science*, **2020**,9(4), 262-280.
[18] E. Amouzad Mahdiraji, N. Ramezani, *International Journal of Science and Engineering Investigations (IJSEI)*, **2020**, 9, 35-42.
[19] E. Amouzad Mahdiraji, N. Ramezani, *Signal Processing and Renewable Energy*, **2020**, 4, 37-50.
[20] A.G. Boulanger, A. Chu, S. Maxx, D. Waltz, *Proc. I EEE*, **2011**. 99, 1116–1138.
[21] E. Amouzad Mahdiraji, N. Ramezani, *International Journal of Science and Engineering Investigations (IJSEI)*, **2020**, 9, 24-28.
[22] O. Sundstrom, C. Binding, *IEEE Trans. Smart Grid*, **2012**, 3, 26–37.
[23] E. Amouzad Mahdiraji, *Signal Processing and Renewable Energy*, **2020**, 4, 67-80.
[24] E. Amouzad Mahdiraji, M. Sedghi Amiri, *Journal of Engineering in Industrial Research*, **2020**, 1, 111-122.
[25] N. Kayedi, A. Samimi, M. Asgari Bajgirani, A. Bozorgian, *South African Journal of Chemical Engineering*, **2021**, *35*, 153-158.
[26] A. Bozorgian, A. Samimi, *International Journal of New Chemistry*, **2021**, *8*, 41-58.
[27] A. Bozorgian, S. Zarinabadi, A. Samimi, *Chemical Methodologies,* **2020**, *4*, 477-493.
[28] F. Zare Kazemabadi, A. Heydarinasab, A. Akbarzadeh, M. Ardjmand, *Artificial Cells, Nanomedicine, and Biotechnology,* **2019**, *47*, 3222-3230.
[29] A. Samimi, *Journal of Engineering in Industrial Research*, **2021,** *2*, 71-76.
[30] F. Zare Kazemabadi, A. Heydarinasab, A. Akbarzadehkhiyavi, M. Ardjmand, *Chemical Methodologies*, **2021**, *5*, 135-152.
[31] S. M. S. Mirnezami, F. Zare Kazemabadi, A. Heydarinasab, *Progress in Chemical and Biochemical Research*, **2021**, *4*, 191-206.
[32] M. Torkaman, F. Zare Kazemabadi, *Oriental Journal of Chemistry*, **2017**, *33*, 1976-1984.
[33] R. Rahimiyan, *Advanced Journal of Chemistry, Section B: Natural Products and Medical Chemistry*, **2020**, *2*, 247-253.
[34] R. Rahimiyan, *Advanced Journal of Chemistry, Section B: Natural Products and Medical Chemistry*, **2020**, *2*, 239-246.
[35] R. Rahimiyan, *Journal of Engineering in Industrial Research*, **2021**, *2*, 95-112.
[36] Y. Raziani, S. Raziani, *Journal of Chemical Reviews*, **2021**, *3*, 83-96.
[37] E. Amouzad Mahdiraji, M. Sedghi Amiri, *Journal of Engineering in Industrial Research*, **2021**, *2*, 7-16.